

Hybrid Mesons

Bernhard Ketzer*

Physik Department, Technische Universität München, D-85748 Garching, Germany

E-mail: Bernhard.Ketzer@tum.de

The $SU(3)_{\text{flavor}}$ constituent quark model has been quite successful to explain the properties as well as the observed spectrum of mesons with pseudoscalar and vector quantum numbers. Many radial and orbital excitations of quark-antiquark ($q\bar{q}'$) systems predicted by the model, however, have not yet been observed experimentally or assigned unambiguously. In addition, a much richer spectrum of mesons is expected from QCD, in which quarks interact with each other through the exchange of colored self-interacting gluons. Owing to this particular structure of QCD, configurations are allowed in which an excited gluonic field contributes to the quantum numbers J^{PC} of the meson. States with a valence color-octet $q\bar{q}'$ pair neutralized in color by an excited gluon field are termed hybrids. The observation of such states, however, is difficult because they will mix with ordinary $q\bar{q}'$ states with the same quantum numbers, merely augmenting the observed spectrum for a given J^{PC} . Since the gluonic field may carry quantum numbers other than 0^{++} , however, this can give rise to states with “exotic” quantum numbers $J^{PC} = 0^{--}, 0^{+-}, 1^{-+}, 2^{+-}, \dots$. The lowest-lying hybrid multiplet is expected to contain a state with exotic quantum numbers $J^{PC} = 1^{-+}$. The identification of such a state is considered a “smoking gun” for the observation of non- $q\bar{q}'$ mesons. The search for hybrid states has been a central goal of hadron spectroscopy in the last 20 years. Ongoing and upcoming high-statistics experiments are expected to shed new light on the existence of such states in nature. In this paper, theoretical predictions for masses and decay modes as well as recent experimental evidence for hybrid meson states and future experimental directions are discussed.

*Sixth International Conference on Quarks and Nuclear Physics,
April 16-20, 2012
Ecole Polytechnique, Palaiseau, Paris*

*Speaker.

1. Introduction

Mesons are experimentally characterized by quantum numbers $I(J^P)$, with the isospin I , the total angular momentum $J = 0, 1, 2, \dots$, and the parity P . Neutral flavorless mesons are eigenstates of the particle-antiparticle conjugation operator and thus have a defined charge conjugation parity C . Flavorless mesons are eigenstates of the G parity. In the constituent quark model, mesons are described as color-singlet bound states of a quark q and an antiquark \bar{q}' . The quantum numbers P , C and G are then given by

$$P = (-1)^{L+1}, \quad C = (-1)^{L+S}, \quad G = (-1)^{L+S+I}, \quad (1.1)$$

where L is the relative orbital angular momentum of q and \bar{q}' , and S the total intrinsic spin of the $q\bar{q}'$ pair, with $S = 0, 1$. This gives rise to meson states with quantum numbers $J^{PC} = 0^{-+}, 0^{++}, 1^{--}, 1^{+-}, 1^{++}, 2^{--}, 2^{-+}, 2^{++}, \dots$

Quantum Chromodynamics (QCD) allows for a much richer spectrum of mesons, including configurations in which an excited gluonic field contributes to the quantum numbers J^{PC} of the meson. States with a valence color-octet $q\bar{q}'$ pair neutralized in color by an excited gluon field are termed hybrids. Since the gluonic field may carry quantum numbers different from those of the vacuum, hybrids can also appear with “exotic” quantum numbers $J^{PC} = 0^{--}, 0^{+-}, 1^{-+}, 2^{+-}, \dots$. The unambiguous identification of resonances with such quantum numbers is considered a “smoking gun” for the observation of mesons beyond the $q\bar{q}'$ configuration. Recent and upcoming high-statistics experiments are about or expected to shed new light on the existence of such states in nature. In this paper theoretical predictions and the present experimental evidence for hybrid meson states are discussed. Directions for and expectations from future experiments are given.

2. Theoretical Predictions

The properties of hadrons are traditionally estimated from phenomenological models like the quark model, the bag model, the flux tube model, QCD sum rules, or effective theories with pions and other pseudoscalar particles as the active degrees of freedom. Recently, also lattice QCD (LQCD) started to make predictions for meson properties like their masses and widths, which can be tested by experiments.

2.1 Models

In the Bag model gluonic excitations correspond to modes of the gluonic field allowed by the boundary conditions on the surface of the bag. The lowest eigenmodes are transverse electric (TE) and transverse magnetic (TM) gluons with quantum numbers $J^{PC} = 1^{+-}$ and 1^{--} , respectively [1]. The lowest-mass hybrid mesons are formed by combining a $q\bar{q}'$ system with spin 0 or 1 with a TE gluon. This yields four nonets with quantum numbers and masses given in Table 1.

Calculations using the QCD spectral sum rule (QSSR) approach favor the 1^{-+} state at a mass between $\lesssim 1.5 \text{ GeV}/c^2$ [10], and $\sim 1.8 \text{ GeV}/c^2$ [11–13]. The latter authors also find a 1^{--} hybrid almost degenerate with the 1^{-+} , while they expect the exotic 0^{--} at a much higher mass of $\sim 2.8 \text{ GeV}/c^2$. Other low-mass hybrids have not been investigated in more detail in the QSSR approach.

Table 1: Quantum numbers and approximate masses of non-strange hybrids in various models. The LQCD masses in parentheses are given for a pion mass of $396 \text{ MeV}/c^2$. $J_{q\bar{q}}^{PC}$ and J_g^{PC} denote the quantum numbers of the $q\bar{q}'$ pair and the gluon, respectively, which couple to give J^{PC} of the hybrid. Bold numbers indicate spin-exotic quantum numbers.

| Model | $J_{q\bar{q}}^{PC}$ | J_g^{PC} | J^{PC} | Mass (GeV/c^2) |
|------------------------------------|---------------------------|---------------|---|---------------------------|
| Bag [2, 3] | 0^{-+} | 1^{+-} (TE) | 1^{--} | ~ 1.7 |
| | 1^{--} | 1^{+-} (TE) | $(0, \mathbf{1}, 2)^{-+}$ | $\sim 1.3, 1.5, 1.9$ |
| | 0^{-+} | 1^{--} (TM) | 1^{+-} | heavier |
| | 1^{--} | 1^{--} (TM) | $(0, \mathbf{1}, 2)^{++}$ | heavier |
| Flux tube [4, 5] | 0^{-+} | 1^{+-} | 1^{--} | 1.7-1.9 |
| | 1^{--} | 1^{+-} | $(0, \mathbf{1}, 2)^{-+}$ | 1.7-1.9 |
| | 0^{-+} | 1^{+-} | 1^{++} | 1.7-1.9 |
| | 1^{--} | 1^{+-} | $(\mathbf{0}, \mathbf{1}, \mathbf{2})^{+-}$ | 1.7-1.9 |
| Constituent gluon [6]/[7] | 0^{-+} | 1^{--} | 1^{+-} | 1.3-1.8 / 2.1 |
| | 1^{--} | 1^{--} | $(0, \mathbf{1}, 2)^{++}$ | 1.3-1.8 / 2.2 |
| | 1^{+-} | 1^{--} | $(0, \mathbf{1}, 2)^{-+}$ | 1.8-2.2 / 2.2 |
| | $(0, \mathbf{1}, 2)^{++}$ | 1^{--} | $1^{--}, (\mathbf{0}, \mathbf{1}, 2)^{--}, (\mathbf{1}, \mathbf{2}, 3)^{--}$ | 1.8-2.2 / 2.3 |
| Constituent gluon / LQCD [8, 9] | 0^{-+} | 1^{+-} | 1^{--} | (2.3) |
| | 1^{--} | 1^{+-} | $(0, \mathbf{1}, 2)^{-+}$ | (2.1, 2.0, 2.4) |
| | 1^{+-} | 1^{+-} | $(0, \mathbf{1}, 2)^{++}$ | (> 2.4) |
| | $(0, \mathbf{1}, 2)^{++}$ | 1^{+-} | $1^{+-}, (\mathbf{0}, \mathbf{1}, \mathbf{2})^{+-}, (\mathbf{1}, \mathbf{2}, 3)^{+-}$ | (> 2.4) |

In the flux tube model gluonic excitations correspond to transverse vibrations of the string-like flux tube between a $q\bar{q}'$ pair. For zero angular momentum, the flux tube behaves as if it has quantum numbers $J_g^{PC} = 0^{++}$, which results in the ordinary quark model meson quantum numbers when combined with the underlying $q\bar{q}'$ system. For one unit of angular momentum, the flux tube quantum numbers can be $J_g^{PC} = 1^{-+}$ or 1^{+-} . The quantum numbers and masses of the gluonic excitations as predicted by the flux tube model are summarized in Table 1.

An alternative description of gluonic excitations suggests to construct Fock states of hadrons from massive constituent quarks and gluons. In the simplest constituent gluon picture, a transverse quasigluon with $J^{PC} = 1^{--}$ is added in a relative S wave to a $q\bar{q}'$ system in an S wave with spin 0 or 1. This gives rise to a supermultiplet of four nonets with the same quantum numbers as P wave $q\bar{q}'$ states, none of them exotic, as shown in Table 1. Predictions for the masses of the non-strange members of these nonets vary considerably between different approaches within the constituent gluon picture.

2.2 Lattice Gauge Theory

Most LQCD studies focused on the exotic 1^{-+} hybrid. A more recent quenched calculation on large lattices, performed with pion masses as light as $320 \text{ MeV}/c^2$ gives a mass of the 1^{-+} exotic of $1.74(25) \text{ GeV}/c^2$ when extrapolated to the physical pion mass [14]. Recently, a fully dynamical (unquenched) calculation of the complete spectrum of light-quark isoscalar and isovector mesons has been performed. The resulting isovector meson spectrum for a pion mass of $700 \text{ MeV}/c^2$ is depicted in Fig. 1 [9]. Quantum numbers and the quark-gluon structure of a meson state n with

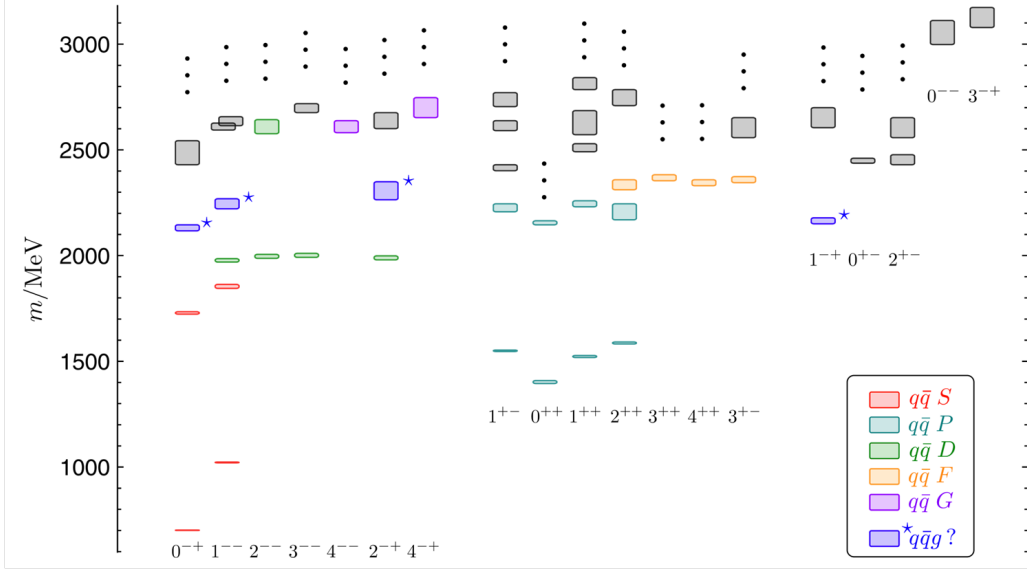


Figure 1: Spectrum of light isovector mesons resulting from a state-of-the-art lattice calculation [9], sorted by their quantum numbers J^{PC} . The box size indicates the statistical uncertainty on the masses. The colors indicate the dominant structure of the states. The pion mass used in these calculations is $700\text{MeV}/c^2$.

a given mass m_n are extracted by studying matrix elements $\langle n|\mathcal{O}_i|0\rangle$, which encode the extent to which operator \mathcal{O}_i overlaps with state n . The dominant operator overlaps are indicated by the colors, and the corresponding operators are indicated in suggestive form in the lower right hand corner of Fig. 1.

In addition to ordinary states consisting of a valence $q\bar{q}$ pair, the calculation also predicts states in which both quark and gluonic degrees of freedom contribute to the quantum numbers (hybrids). The lowest-lying isovector hybrid states form a super-multiplet consisting of a spin-exotic state with $J^{PC} = 1^{-+}$, and three non-exotic states with quantum numbers 0^{-+} , 1^{-+} , and 2^{-+} .

It is interesting to note that none of the models described in Sec. 2.1 is able to reproduce the degeneracy pattern of hybrid states emerging from LQCD. Considering a model, in which a constituent gluon couples to a $q\bar{q}$ pair in a P wave rather than in an S wave as above, such that $J^{PC} = 1^{+-}$, one is able to successfully reproduce the pattern of hybrid states from LQCD [8, 9], as shown in Table 1.

2.3 Decay Modes

In order to clarify the nature of a non- $q\bar{q}'$ resonance, it is important to study its decay properties and compare them to theoretical predictions. Hybrid meson decays have been studied in models [15–17] as well as, recently, in LQCD [18]. The results are summarized in Table 2 for low-mass hybrids with $J^{PC} = 1^{-+}, 0^{-+}, 1^{-+}, 2^{-+}$.

Table 2: Total widths in MeV/c^2 and dominant decay channels of light isovector hybrid mesons according to model calculations and LQCD. Values labeled IKP [15] and PSS [17] are for a hybrid mass of $1.8\text{ GeV}/c^2$. Results for the IKP model have been calculated in [17]. LQCD [18] results are for a hybrid mass of $2.0\text{ GeV}/c^2$.

| J^{PC} | Total width (MeV/c^2) | | | Dominant channels |
|----------|----------------------------------|----------|-----------|---|
| | IKP [15] | PSS [17] | LQCD [18] | |
| 1^{-+} | 117 | 81 | 180 | $b_1(1235)\pi, f_1(1285)\pi, \rho\pi, \eta(1295)\pi, a_1(1260)\eta$ |
| 0^{-+} | 132 | 102 | | $f_0(1370)\pi, \rho\pi, \rho(1450)\pi, K^*K$ |
| 1^{--} | 112 | 70 | | $a_1(1260)\pi, a_2(1320)\pi, \omega\pi, K_1(1270)K, \rho\eta$ |
| 2^{-+} | 59 | 27 | | $f_2(1270)\pi, b_1(1235)\pi, \rho\pi$ |

3. Experiments

Experimental evidence for the existence of hybrid mesons can come from two sources. The observation of an overpopulation of states with $q\bar{q}'$ quantum numbers may indicate the existence of states beyond the quark model, i.e. hybrids, glueballs or multi-quark states. The densely populated spectrum of light mesons in the mass region between 1 and $2\text{ GeV}/c^2$, and the broad nature of the states involved, however, makes this approach difficult. The identification of a resonance with exotic quantum numbers, however, is a clear evidence for the existence of such states. Unfortunately, models and LQCD predictions do not agree on the quantum numbers and masses expected for the lowest-mass hybrids (c.f. Sec. 2). It is thus of great importance for our understanding of non-perturbative QCD to test those predictions experimentally.

3.1 Production Mechanisms

Production experiments, where the total energy is shared between a multi-meson final state X and a recoil particle, can be employed to produce both non-exotic and exotic states. The quantum numbers of the multi-meson system are restricted only by conservation laws of the reaction. The final state will contain contributions from all (indistinguishable) intermediate states with different quantum numbers. A partial wave analysis is usually required to disentangle the different contributions. The decay of a resonance into a multi-particle final state is commonly described in the isobar model, which assumes a series of sequential two-body decays into intermediate resonances (isobars), which eventually decay into the final state observed in the experiment. A partial wave is characterized by a set of quantum numbers $J^{PC}M^\epsilon R_1 R_2 \begin{bmatrix} L \\ S \end{bmatrix}$; M is the absolute value of the spin projection onto the z -axis; ϵ is the reflectivity; L is the orbital angular momentum between the isobars R_1 and R_2 , and S their total spin.

The most prominent production reactions are shown in Fig. 2. Diffractive excitation (2a) of an incoming beam particle (usually a pion or a kaon) proceeds via the exchange of a Regge trajectory R in the t -channel. Angular momentum as well as 4-momentum t is exchanged. Instead of t , the positive variable $t' = |t| - |t|_{\min}$, is often used, where $|t|_{\min}$ is the minimum value of $|t|$ which is needed by kinematics to produce a final state X of a given mass. Antiproton annihilation (2b) can proceed either in flight or at rest, and on protons or on neutrons. For $\bar{p}p$, the initial state is a mixture of isospin $I = 0$ and 1, with $I_3 = 0$, while for $\bar{p}n$ the initial state is pure $I = 1$. Photoproduction

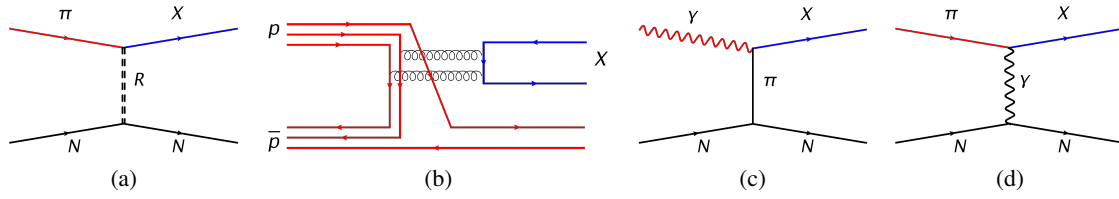


Figure 2: Production mechanisms of hybrid mesons.

proceeds via real or quasi-real virtual photons. Using a beam of real photons (2c) with quantum numbers $J^{PC} = 1^{--}$, the production of spin-exotic hybrids with $S = 1$ is expected to be favored from Vector Meson Dominance, compared to diffractive production from a pion beam with $J^{PC} = 0^{-+}$ and $S = 0$. This hypothesis can also be tested using quasi-real photons (2d) from the Coulomb field of a heavy target nucleus. In addition, hard exclusive lepton production was also proposed as a tool to study a 1^{-+} hybrid [19].

3.2 Hybrids with Exotic Quantum Numbers

Models as well as LQCD consistently predict the lightest spin-exotic hybrid to have quantum numbers $J^{PC} = 1^{-+}$. Currently, there are three experimental candidates for a light 1^{-+} hybrid [20]: the $\pi_1(1400)$ and the $\pi_1(1600)$, observed in diffractive reactions and $\bar{p}N$ annihilation, and the $\pi_1(2015)$, seen only in diffraction. The resonant nature of these states is still heavily disputed in the community (for a recent review, see [21]). New experiments with higher statistics and better acceptance, allowing for more elaborate analysis techniques, are needed in order to shed new light on these questions.

3.2.1 Diffractive Production

The COMPASS experiment [22] at CERN's Super Proton Synchrotron (SPS) is a large-acceptance, high-resolution magnetic spectrometer, which is gathering high-statistics event samples of diffractive and Coulomb production reactions of hadronic beam particles into final states containing charged and neutral particles.

3π Final State

In a first analysis of 420k events of the $\pi^- \pi^- \pi^+$ final state from scattering of $190 \text{ GeV}/c$ π^- on a Pb target with 4-momentum transfer $0.1 < t' < 1.0 \text{ GeV}^2/c^2$, a clear signal in the $1^{-+} 1^+ \rho \pi P$ partial wave has been observed [23], as shown in Fig. 3a. The data points are the results of independent extended maximum likelihood fits of production amplitudes to angular distributions in bins of the 3π mass, including 41 partial waves and a flat background wave. The curves show a fit of Breit-Wigner resonances (blue dashed) and a coherent background (magenta dotted) to the spin-density matrix. The phase differences between the exotic wave and the $1^{++} 0^+ \rho \pi S$ and the $2^{-+} 0^+ f_2 \pi S$ waves have been examined. While the latter appears to be rather flat, the former, shown in Fig. 4a, clearly shows an increase around $1.7 \text{ GeV}/c^2$, suggesting a resonant contribution to the 1^{-+} wave. Although allowed in the model, no significant intensity was found in the negative-reflectivity spin-exotic wave.

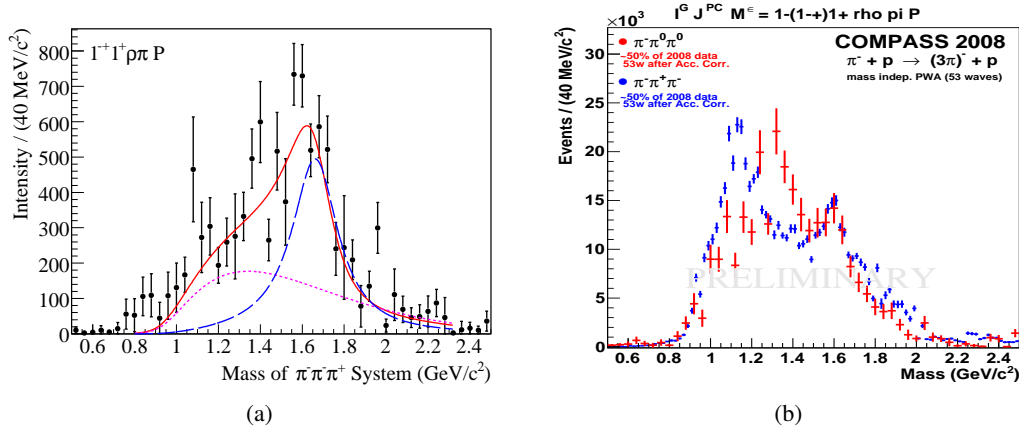


Figure 3: Intensity of exotic $1^{-+}1^{+}\rho\pi P$ wave as a function of 3π invariant mass for 4-momentum transfer between 0.1 and $1.0\text{GeV}^2/c^2$, (a) for Pb target and $\pi^{-}\pi^{-}\pi^{+}$ final state, (b) for H target and charged (blue) and neutral (red) 3π final states.

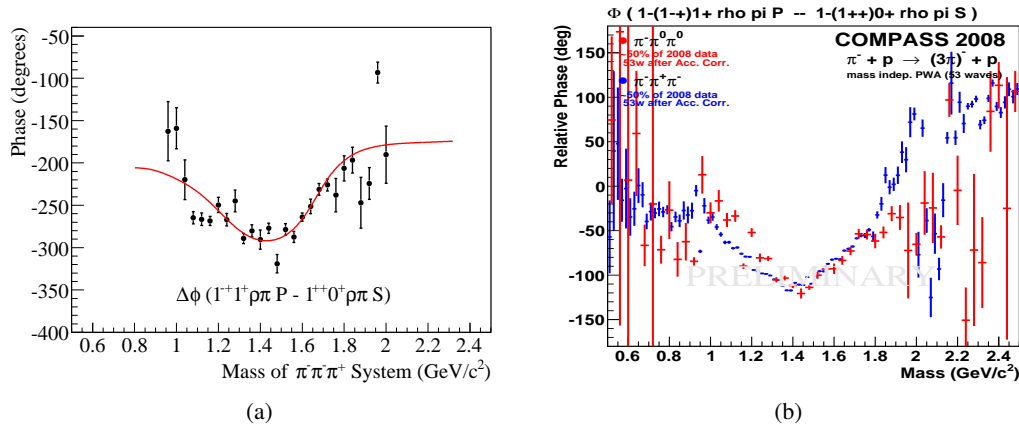


Figure 4: Phase difference between the $1^{-+}1^{+}\rho\pi P$ and the $1^{++}0^{+}\rho\pi S$ waves, (a) for Pb target and $\pi^{-}\pi^{-}\pi^{+}$ final state, (b) for H target and charged (blue) and neutral (red) 3π final states.

A much bigger data set was taken by COMPASS with a liquid hydrogen target, surpassing the existing world statistics by a factor of more than 20. In addition to the $\pi^{-}\pi^{-}\pi^{+}$ final state with approximately 100M events [24], also the one containing neutral pions, $\pi^{-}\pi^{0}\pi^{0}$, with more than 2.4M events has been analyzed [25]. Figure 3b shows the intensity in the exotic wave for both final states, where the intensity in the $2^{++}1^{+}\rho\pi D$ wave was used to normalize the two data sets. A set of 53 waves including a flat wave was used to account for the increase of statistics. Similarly to the Pb target, a peak structure is observed between 1.6 and $1.7\text{GeV}/c^2$ for the H target. The phase difference to the 1^{++} wave, shown in Fig. 4b for the H target, also exhibits a clear rising variation, consistent with a resonant interpretation of the peak. The structures at lower masses, visible for

the H target, were found to be unstable and largely depending on the fit model. The intensity in the peak structure at $1.67 \text{ GeV}/c^2$ appears to be enhanced with respect to the broad remaining non-resonant background for the Pb target compared to the H target. This observation is consistent with a general enhancement of the intensity of waves with spin projection $M = 1$ and a corresponding reduction of waves with $M = 0$ for the Pb target, observed also for the dominant 1^{++} and 2^{-+} waves [24]. For the H target, no fit of the spin density matrix has yet been performed.

In order to better understand the background, non-resonant processes like the Deck effect [26] have to be taken into account in the fit model. As a first step, pure Deck-like events were generated, and the events were passed through the Monte-Carlo simulation framework of the experiment and were reconstructed and analyzed in the same way as real experimental data. The intensity appearing in the spin-exotic $1^{-+}1^+ \rho\pi P$ wave was found to reproduce both the intensity and the shape of the low-mass background in Fig. 3, indicating a large non-resonant contribution to the observed $1^{-+}1^+ \rho\pi P$ wave. Pure Deck-like events, however, do not exhibit any enhancement between 1.6 and $1.7 \text{ GeV}/c^2$, nor any significant phase motion. A complete analysis is under way, which includes the Deck amplitude in the fit to the spin density matrix, and hence allows for interferences between resonant and non-resonant amplitudes.

$\eta\pi$ and $\eta'\pi$ Final States

COMPASS has also analyzed data for $\eta\pi$ ($\eta \rightarrow \pi^+\pi^-\pi^0$) and $\eta'\pi$ ($\eta' \rightarrow \pi^+\pi^-\eta$, $\eta \rightarrow \gamma\gamma$) final states from diffractive scattering of $190 \text{ GeV}/c$ π^- off a H target [27]. In total, about 116k events were collected for the first final state, and about 39k events for the second, exceeding the statistics of previous experiments by more than a factor of 5. Four waves with natural parity exchange, $1^{-+}1^+$ (P wave, exotic), $2^{++}1^+/2^+$ (D wave), and $4^{++}1^+$ (G wave), were included in the fit, together with a flat background added incoherently. Waves with unnatural parity exchange were also included, but remained compatible with zero up to masses of about $2.5 \text{ GeV}/c^2$. Figures 5a and 5b show the intensities in the $2^{++}1^+$ and $1^{-+}1^+$ waves for the $\eta'\pi$ (black data points) and the $\eta\pi$ final state (red data points), respectively. Here, the data points for the latter final state have been scaled by a phase-space factor $(q'/q)^{J+1/2}$, with $q^{(l)}$ being the breakup momentum into $\eta^{(l)}\pi$ at a given invariant mass. While the intensities in the D wave (as well as in the G wave, not shown here) are remarkably similar in intensity and shape in both final states after normalization, the P wave intensity appears to be very different. For $\eta\pi$, it is strongly suppressed, while for $\eta'\pi$ it is the dominant wave. The phase differences between the $2^{++}1^+$ and the $1^{-+}1^+$ waves are displayed in Fig. 5c for the two final states. For masses below $1.4 \text{ GeV}/c^2$ the phase differences agree for the two final states, showing a rising behavior due to the resonating D wave. For higher masses, the phase differences evolve quite differently, suggesting a different resonant contribution in the two final states. As for the 3π final states, both resonant and non-resonant contributions to the exotic wave have to be included in a fit to the spin-density matrix in order to describe both intensities and phase shifts [27]. Regardless of this, the spin-exotic contribution to the total intensity is found to be much larger for the $\eta'\pi$ final state than for the $\eta\pi$ final state, as expected for a hybrid candidate.

3.2.2 Photoproduction

The CEBAF Large Acceptance Spectrometer (CLAS) [28] at Hall B of Jefferson Laboratory is studying photo- and electro-induced hadronic reactions by detecting final states containing charged

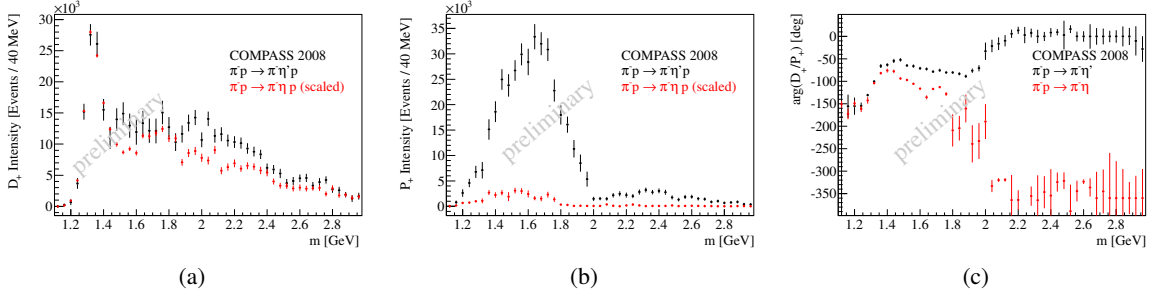


Figure 5: Comparison of waves for $\eta\pi$ (red data points) and $\eta'\pi$ (black data points) final states. (a) Intensity of the $J^{PC} = 2^{++}$ D wave, (b) intensity of the spin-exotic 1^{-+} P wave, (c) phase difference between D and P wave.

and neutral particles. Two experimental campaigns in 2001 and 2008 were dedicated to the search for exotic mesons photoproduced in the charge exchange reaction $\gamma p \rightarrow \pi^+ \pi^+ \pi^- (n)$ (see Fig. 2c). A tagged-photon beam produced from an electron beam with energies up to 5.75 GeV was impinging on an 18cm long liquid hydrogen target. In order to increase the acceptance for meson production, the target was shifted upstream by 1 m and the toroidal magnetic field was reduced to half its nominal value. Charged particles were detected by a toroidal spectrometer equipped with drift chambers and identified by a time-of-flight detector. Events with three outgoing pions were selected by vertex and timing cuts. The recoiling neutron was identified through its missing mass. The first campaign resulted in a set of 83k events subjected to a partial wave analysis [29]. No evidence for a 1^{-+} exotic state, nor for the 1^{++} state was found. The second data taking period yielded a much larger data set of 520k events for the PWA [30], after the background from baryon resonances in the target vertex had been removed by cuts on 4-momentum transfer $t' < 0.105 \text{ GeV}^2/c^2$ and on the laboratory angle of both π^+ , $\theta_{\text{lab}}(\pi^+) \leq 25^\circ$, to select peripheral events with forward-going pions. The PWA included 19 waves with $J^{PC} = 1^{++}$, 2^{++} , 1^{-+} , and 2^{-+} , and a flat background wave. Helicity conservation forbids the production of waves with $M = 0$, and hence $J = 0$, for an incoming photon and pion exchange. Waves with $M^e = 1^\pm$ are expected to be populated equally as a result of ambiguities. Evidence was found for the $a_1(1260)$, the $a_2(1320)$ and the $\pi_2(1670)$ in the $1^{++}1^\pm \rho\pi S$ wave, the $2^{++}1^\pm \rho\pi D$ wave and the $2^{-+}1^\pm f_2\pi S$ wave, respectively. A non-negligible population of the $M = 0$ spin projection of the 1^{++} and 2^{-+} waves, however, indicates a possible leakage or non-resonant S wave production via the Deck effect. The intensity of the exotic $1^{-+}1^\pm \rho\pi P$ wave, shown in Fig. 6a as a function of the 3π invariant mass, does not exhibit any evidence for structures around $1.7 \text{ GeV}/c^2$. The fluctuations at masses above $1.8 \text{ GeV}/c^2$ are not understood yet. Its phase difference relative to the $2^{-+}1^\pm f_2\pi S$ wave, displayed in Fig. 6b, shows a continuous downward trend in the relevant mass region, as expected for a 2^{-+} resonance subtracted from a non-resonant background (blue line). The conclusion from the CLAS experiments is that there is no evidence for an exotic 1^{-+} wave in photoproduction, with an upper limit of 2% of the total intensity.

The COMPASS experiment studied pion-induced reactions on a Pb target at very low values of 4-momentum transfer, $t' < 0.001 \text{ GeV}^2/c^2$, which can proceed both diffractively via the exchange

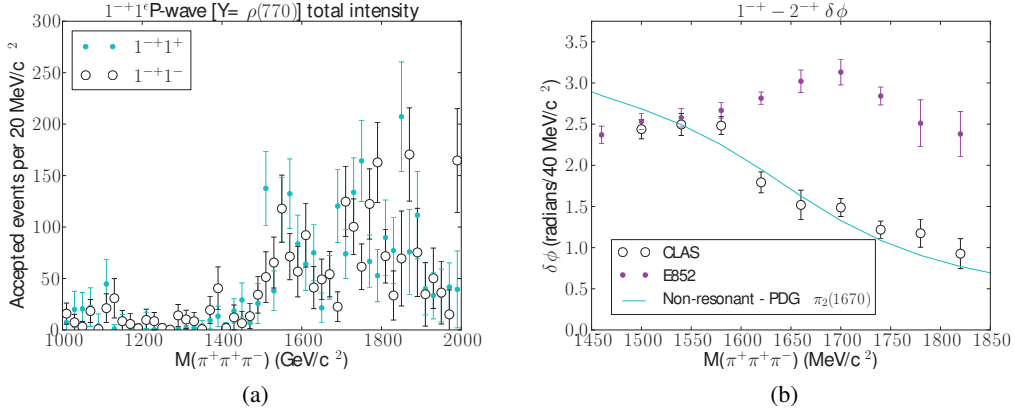


Figure 6: The $1^{-+}1^{\pm} \rho\pi P$ waves from photoproduction at CLAS [30]. (a) Intensities as a function of 3π invariant mass, (b) phase difference to the $2^{-+}1^{\pm} f_2\pi S$ wave, with the corresponding result from diffractive production at E852 [31] overlaid.

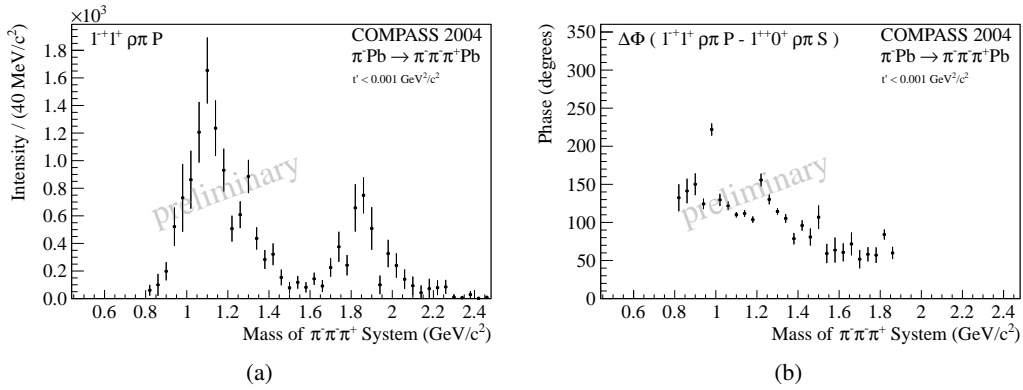


Figure 7: The $1^{-+}1^{\pm} \rho\pi P$ waves from photoproduction at COMPASS. (a) Intensity vs. 3π invariant mass, (b) phase relative to the $1^{++}0^+ \rho\pi S$ wave.

of a Pomeron and via the exchange of quasi-real photons from the Coulomb field of the heavy nucleus (see Fig. 2d). A partial wave analysis of this data set consisting of approximately 1M events was performed using a total of 37 waves, showing no sign of a resonance in the $1^{-+}1^{\pm} \rho\pi P$ wave at a mass of $1.7\text{GeV}/c^2$ (c.f. Fig. 7), consistent with the CLAS observation.

3.3 Non-exotic Hybrids

While there is some evidence for an isovector member of a light 1^{-+} exotic nonet, as detailed in Sec. 3.2.1, members of non-exotic multiplets will be more difficult to identify. Most of the light meson resonances observed until now are in fact compatible with a $q\bar{q}'$ interpretation. Taking the LQCD predictions as guidance, the lowest isovector hybrids with ordinary quantum numbers

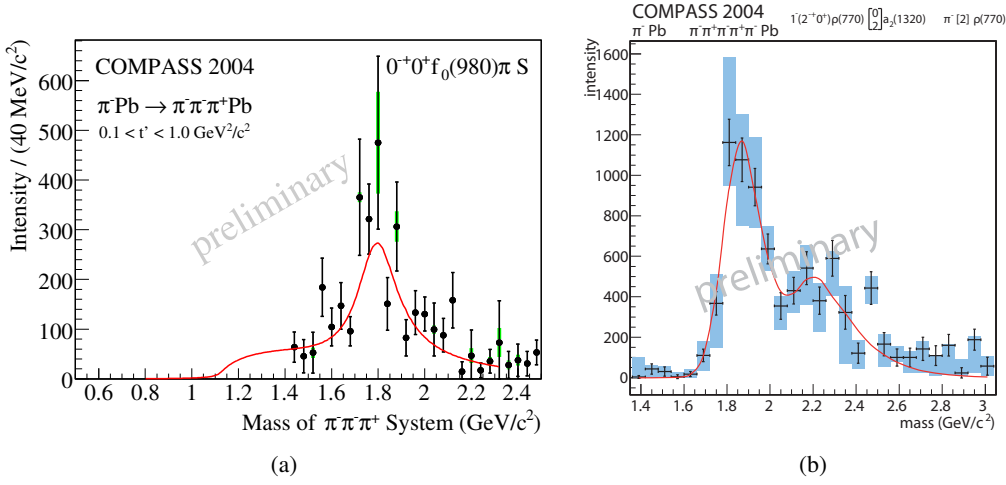


Figure 8: Intensities of (a) the $0^{-+}0^{+} f_0(980)\pi S$ wave in the 3π final state, and (b) the $2^{-+}0^{+} \rho a_2(1320)[\rho\pi]D$ wave in the 5π final state, both from a Pb target.

Table 3: Mass and width of the $\pi(1800)$ and $\pi_2(1880)$, obtained from recent partial wave analyses of the COMPASS experiment.

| Resonance | $J^{PC}M^e$ [channel] L | Mass (MeV/ c^2) | Width (MeV/ c^2) | Events |
|---------------|--|-------------------------|--------------------------|--------|
| $\pi(1800)$ | $0^{-+}0^{+} f_0(980)\pi S$ | $1785 \pm 9^{+12}_{-6}$ | $208 \pm 22^{+21}_{-37}$ | 420k |
| | $0^{-+}0^{+} f_0(1500)[\rho\rho]\pi S$ | $1781 \pm 5^{+1}_{-6}$ | $168 \pm 9^{+5}_{-14}$ | 200k |
| $\pi_2(1880)$ | $2^{-+}0^{+} \rho a_2(1320)[\rho\pi]D$ | $1854 \pm 6^{+6}_{-4}$ | $259 \pm 13^{+13}_{-17}$ | 200k |

should have $J^{PC} = 0^{-+}, 1^{--},$ and 2^{-+} (see Sec. 2.2). We will review the latest observations concerning resonances with these quantum numbers.

The $\pi(1800)$

There is clear experimental evidence for the $\pi(1800)$ [20]. The latest measurements of this state come from the COMPASS experiment, using a 190 GeV/ c π^{-} beam impinging on a Pb target. Figure 8a shows the intensity in the dominant 0^{-+} wave determined from a partial wave analysis of the 3π final state. A strong $\pi(1800)$ signal was recently also observed in an analysis of the 5π final state from COMPASS [32]. Table 3 summarizes the masses and widths obtained by fitting Breit-Wigner functions to the spin density matrix. The interpretation of the experimental decay pattern is not straightforward. On the one hand, it prefers to decay into a pair of $L = 1$ and $L = 0$ mesons, as expected for a hybrid (c.f. Sec. 2.3 and Table 2)). Large partial widths for $f_0\pi$ decays, as expected for a hybrid state, have been observed by COMPASS and others [20]. The decay of a $3S q\bar{q}'$ state into this final state should be small. On the other hand, both the hybrid and $q\bar{q}'$ state are predicted to have a sizable $\rho\pi$ partial width, which is not seen. More statistics and advanced coupled-channel analyses are certainly needed to clarify the situation.

The $\pi_2(1880)$

There is growing experimental evidence for the existence of this state. The latest high-statistics

measurements of this state again come from COMPASS. A clear peak is observed in the intensity of the $2^{-+}0^{+} f_2\pi D$ wave for both a Pb and a H target [24], which is shifted in mass with respect to the $\pi_2(1670)$, and also exhibits a phase motion relative to the latter in the $f_2\pi S$ wave. This observation, however, was also explained differently, including e.g. the interference of the $f_2\pi S$ wave with a Deck-like amplitude, which shifts the true π_2 peak to lower masses [33]. For 5π final states [32], a total of three resonances are needed to describe the 2^{-+} sector, the $\pi_2(1670)$, the $\pi_2(1880)$, and a high-mass $\pi_2(2200)$. Figure 8b shows the intensity in the $2^{-+}0^{+} \rho a_2(1320)[\rho\pi]D$ wave, together with a fit of three Breit-Wigner functions to the spin-density matrix. The resulting mass and width deduced from this fit are given in Table 3.

States with $J^{PC} = 1^{--}$

The PDG lists two ρ -like excited states, the $\rho(1450)$ and the $\rho(1700)$, observed in e^+e^- annihilation, photoproduction, antiproton annihilation and τ decays [20]. Their masses are consistent with the 2^3S_1 and $1^3D_1 q\bar{q}'$ states, respectively, but their decay patterns do not follow the 3P_0 rule [34]. The existence of a light vector hybrid state, mixing with the $q\bar{q}'$ states, was proposed to solve these discrepancies [35]. Recently, BaBar has reported the observation of a 1^{--} state decaying to $\phi\pi^0$ [36], the $\rho(1570)$. Interpretations of this signal include a new state, a threshold effect, and an OZI-suppressed decay of the $\rho(1700)$. In conclusion, there is no clear evidence for a hybrid state with vector quantum numbers. A clarification of the nature of the ρ -like states, especially above $1.6\text{ GeV}/c^2$, requires more data.

3.4 Heavier Candidates

To avoid experimental difficulties in the light quark sector due to the high density of ordinary $q\bar{q}'$ states below $2.5\text{ GeV}/c^2$, a search for hybrids in the less populated charmonium mass region is expected to be very rewarding. Model calculations as well as LQCD predict the ground state of the charmonium hybrid at a mass of around $4.3\text{ GeV}/c^2$ with exotic quantum numbers 1^{-+} [15, 37, 38]. No candidate state with such quantum numbers, however, has been identified experimentally until now, although many new and yet unexplained states containing charm and bottom quarks have been discovered (for a recent review, see e.g. [39]). Anomalous decay properties and an apparent overpopulation with respect to expectations for $c\bar{c}$ states suggested a non- $q\bar{q}$ nature of $Y(4260)$ state, a 1^{--} state discovered by BaBar in initial state radiation (ISR) [40]. Possible interpretations range from a tetraquark system to a charmonium hybrid. The $Y(2175)$, also discovered by BaBar in ISR [41], has a decay pattern which is strikingly similar to the $Y(4260)$ and the $Y(10860)$, and was therefore discussed as the strangeonium hybrid partner of the $Y(4260)$ [42, 43]. There is, however, no overpopulation of states in the $s\bar{s}$ sector, so radial and orbital excitations have to be considered as well.

4. Conclusions and Outlook

The self-interacting nature of the gluons in QCD allows excitations of the gluonic field, which confines quarks inside mesons, to contribute to the quantum numbers of hadrons. Models of QCD predict the lowest-lying hybrid states at masses varying between 1.3 and $2.2\text{ GeV}/c^2$, and with different quantum numbers and excitation patterns. Recently, a fully unquenched LQCD calculation

yielded predictions for the complete spectrum of isovector mesons made of light quarks, including a light hybrid supermultiplet with quantum numbers $J^{PC} = 0^{-+}, 1^{--}, 2^{-+}$, and a spin-exotic 1^{-+} .

The experimental observation of hybrid mesons thus constitutes a stringent test of non-perturbative QCD. They can be identified either by an overpopulation of states in a given mass region with respect to quark model expectations, or by the detection of states with exotic quantum numbers. A final proof of their nature of course can only come from the observation of the decay pattern and from branching ratios, which are expected to be different for hybrids from the one of ordinary mesons, and from the identification of isoscalar, isovector, and strange members of a multiplet. In addition, the production mechanism is an important question which can be clarified only by studying the systems using different probes and at different energies, employing polarization variables where possible.

The COMPASS experiment has provided clear evidence for the presence of a spin-exotic wave with quantum numbers $J^{PC} = 1^{-+}$ in $\rho\pi$ and $\eta'\pi$ final states in diffractive production from a 190 GeV/c pion beam, consistent with the $\pi_1(1600)$, although non-resonant production seems to be playing an important role. CLAS as well as COMPASS have shown that photoproduction of a 1^{-+} hybrid does not occur with the expected strength. By studying the reaction $\gamma p \rightarrow \pi^- \pi^+ \pi^+(n)$, CLAS has set an upper limit for the 1^{-+} wave of 2% of the total intensity, suggesting that the production of the $\pi_1(1600)$ proceeds via Pomeron exchange, but is suppressed in charged-pion exchange photoproduction. This conjecture calls for a better understanding of the production mechanism, e.g. by analyzing its dependence on 4-momentum transfer or center-of-mass energy.

In addition to the spin-exotic $\pi_1(1600)$, there are candidates for supernumerary states with ordinary quantum numbers 0^{-+} and 2^{-+} , the $\pi(1800)$ and the $\pi_2(1880)$, respectively. Both states have been observed in the past, with new evidence coming from COMPASS in 3π and 5π final states. These states would account for the full set of light hybrid states with the $q\bar{q}'$ pair in $S = 1$ configuration, as predicted from LQCD and quasiparticle models. Candidates for additional states in the ρ -like sector, which could make up the spin-singlet member of the supermultiplet, have been observed at e^+e^- machines, but require confirmation.

New hadron spectroscopy experiments are on the horizon, which are expected to considerably advance our understanding of the meson spectrum. Key features of these experiments will be high statistics requiring highest possible luminosities and sensitivity to production cross sections in the sub-nanobarn region. This can only be achieved by hermetic detectors with excellent resolution and particle identification capabilities, providing a very high acceptance for charged and neutral particles. BESIII at the BEPC-II e^+e^- collider in Beijing has already started to take data in the τ -charm region at a luminosity of $10^{33} \text{ cm}^{-2} \text{ s}^{-1}$, with a maximum center-of-mass energy of 4.6 GeV. At Super-B factories, aiming at a 100-fold luminosity increase to values of $\sim 10^{36} \text{ cm}^{-2} \text{ s}^{-1}$, the sensitivity for new states in the charm and bottom sector will increase dramatically. GlueX is a new experiment which will study photoproduction of mesons with masses below $3 \text{ GeV}/c^2$ at the 12 GeV upgrade of CEBAF, Jefferson Laboratory. An important advantage of the experiment will be the use of polarized photons, which narrows down the possible initial states and gives direct information on the production process. PANDA, a new experiment at the FAIR antiproton storage ring HESR, is designed for high-precision studies of the hadron spectrum in the charmonium mass range. It is expected to run at center-of-mass energies between 2.3 and 5.5 GeV with a maximum luminosity of $2 \cdot 10^{32} \text{ cm}^{-2} \text{ s}^{-1}$.

References

- [1] R. Jaffe and K. Johnson, Phys. Lett. B **60**, 201 (1976).
- [2] M. S. Chanowitz and S. R. Sharpe, Nucl. Phys. B **222**, 211 (1983).
- [3] T. Barnes, F. Close, and F. de Viron, Nucl. Phys. B **224**, 241 (1983).
- [4] N. Isgur and J. E. Paton, Phys. Rev. D **31**, 2910 (1985).
- [5] T. Barnes, F. Close, and E. Swanson, Phys. Rev. D **52**, 5242 (1995).
- [6] S. Ishida, H. Sawazaki, M. Oda, and K. Yamada, Phys. Rev. D **47**, 179 (1993).
- [7] I. J. General, S. R. Cotanch, and F. J. Llanes-Estrada, Eur.Phys.J. **C51**, 347 (2007).
- [8] P. Guo *et al.*, Phys. Rev. D **77**, 056005 (2008).
- [9] J. J. Dudek, Phys. Rev. D **84**, 074023 (2011).
- [10] I. Balitsky, D. Diakonov, and A. Yung, Z. Phys. C **33**, 265 (1986).
- [11] J. Latorre, P. Pascual, and S. Narison, Z. Phys. C **34**, 347 (1987).
- [12] K. G. Chetyrkin and S. Narison, Phys. Lett. B **485**, 145 (2000).
- [13] S. Narison, Phys. Lett. B **675**, 319 (2009).
- [14] J. Hedditch *et al.*, Phys. Rev. D **72**, 114507 (2005).
- [15] N. Isgur, R. Kokoski, and J. E. Paton, Phys. Rev. Lett. **54**, 869 (1985).
- [16] F. E. Close and P. R. Page, Nucl. Phys. B **443**, 233 (1995).
- [17] P. R. Page, E. S. Swanson, and A. P. Szczepaniak, Phys. Rev. D **59**, 034016 (1999).
- [18] C. McNeile and C. Michael, Phys. Rev. D **73**, 074506 (2006).
- [19] I. Anikin *et al.*, Phys.Rev. **D71**, 034021 (2005).
- [20] J. Beringer *et al.*, Phys. Rev. D **86**, 010001 (2012).
- [21] C. A. Meyer and Y. Van Haarlem, Phys. Rev. C **82**, 025208 (2010).
- [22] P. Abbon *et al.*, Nucl. Instr. Meth. A **577**, 455 (2007).
- [23] M. Alekseev *et al.*, Phys. Rev. Lett. **104**, 241803 (2010).
- [24] F. Haas, AIP Conf.Proc. **1374**, 273 (2011).
- [25] F. Nerling, arXiv:1208.0474 [hep-ex] (2012).
- [26] R. T. Deck, Phys. Rev. Lett. **13**, 169 (1964).

- [27] T. Schlüter, D. Ryabchikov, W. Dünneweber, and M. Faessler, PoS **QNP2012**, 074 (2012).
- [28] B. Mecking *et al.*, Nucl.Instrum.Meth. **A503**, 513 (2003).
- [29] M. Nozar *et al.*, Phys. Rev. Lett. **102**, 102002 (2009).
- [30] C. Bookwalter, arXiv:1108.6112 [hep-ex] (2011).
- [31] S. U. Chung *et al.*, Phys. Rev. D **65**, 072001 (2002).
- [32] S. Neubert, AIP Conf. Proc. **1257**, 298 (2010).
- [33] J. Dudek and A. Szczepaniak, AIP Conf. Proc. **814**, 587 (2006).
- [34] T. Barnes, F. Close, P. Page, and E. Swanson, Phys. Rev. D **55**, 4157 (1997).
- [35] A. Donnachie and Y. Kalashnikova, Phys. Rev. D **60**, 114011 (1999).
- [36] B. Aubert *et al.*, Phys. Rev. D **77**, 092002 (2008).
- [37] P. Chen, X. Liao, and T. Manke, Nucl. Phys. Proc. Suppl. **94**, 342 (2001).
- [38] K. J. Juge, J. Kuti, and C. Morningstar, AIP Conf. Proc. **688**, 193 (2003).
- [39] N. Brambilla *et al.*, Eur. Phys. J. C **71**, 1534 (2011).
- [40] B. Aubert *et al.*, Phys. Rev. Lett. **95**, 142001 (2005).
- [41] B. Aubert *et al.*, Phys. Rev. D **74**, 091103 (2006).
- [42] G.-J. Ding and M.-L. Yan, Phys. Lett. B **657**, 49 (2007).
- [43] S.-L. Zhu, Int.J.Mod.Phys. **E17**, 283 (2008).